Experimental Report

Proposal: **9-12-344** **Council:** 10/2012

Title: Kinetic studies of the Trost ligand particpating in a catalytic cycle

This proposal is a new proposal

Researh Area: Chemistry

Main proposer: **EASTOE Julian**

Experimental Team: RACYS Daugirdas
JAMES Craig
ALEXANDER Shirin

Local Contact: GRILLO Isabelle

Samples: Pd - Trost ligand - THF - substrates (organic chemicals) - see figure 1

Instrument	Req. Days	All. Days	From	To
D33	1	1	30/04/2013	01/05/2013

Abstract:

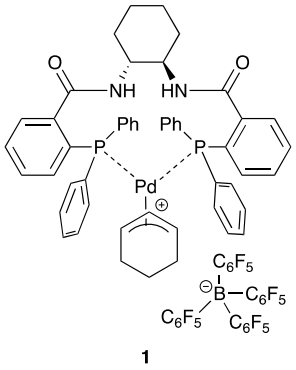
The aim is use time-resolved SANS to monitor the changes in aggregation structure of the Trost ligand[1] Pd-catalyst [(DACH-phenyl-TSL)Pd+(ç3-C6H9)]BArF- 1 (Figure 1 left) in situ whilst it is participating in a catalytic cycle. The experiments will help to reveal further important details of Pd-Trost ligand oligomer structure for (1)n whilst participating in a catalytic cycle. This will provide valuable information for taming this system so that its power can be reliably and reproducibly harnessed for synthesis.

ILL-D33 Report

Trost ligand-Palladium catalyst dynamic reaction analysis

Daugirdas Tomas Racys, Julian Eastoe, Guy C. Lloyd-Jones

Introduction



1

Trost ligand-palladium catalyst **1** facilitates one of the most selective and efficient pathways to carry out allylic alkylation in organic synthesis. However, the catalyst monomeric form **1** may oligomerise even at slightly elevated concentration in solution, which may negatively affect the rate and selectivity of the catalysed reactions, ***Figure 1***. Both catalyst **1** forms may exist in equilibrium and are distinctly apparent in ^{31}P NMR spectra. While the spectroscopic analytical technique does not provide any structural details of the oligomeric architecture, the recent SANS tests suggested that Trost ligand palladium **1** may form unidirectional cylinders consisting of stacked small cyclic oligomeric units in THF. The experimentally measured cylinder diameter and the recent molecular mechanics simulation results are consistent with the formation of stacked cyclic palladium-trost ligand tetramers $\mathbf{((1)_4)_n}$.

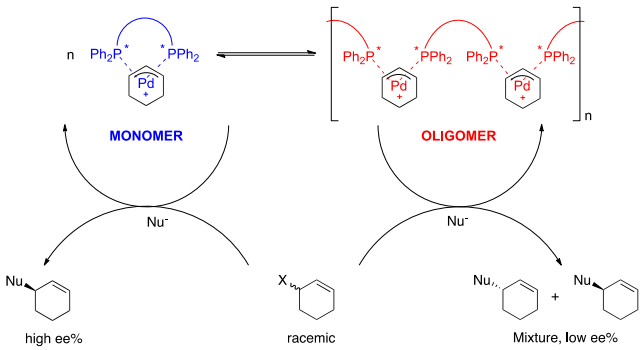


Figure 1. Aggregation of 1 negatively affects the allylic alkylation reaction enantio-selectivity

The levels of aggregation are different across the range of solvents. In low dielectric constant, ε_r, environments the phosphorus NMR data indicate that the least favourable solvent for aggregation is THF. At higher ε_r the multiplet system corresponding to the oligomeric complex $\mathbf{((1)_4)_n}$ is replaced with a system of doublet of doublets indicating a different aggregate architecture.

The neutron scattering tests in several other solvents and solvent mixtures indicated that the cylinders $\mathbf{((1)_4)_n}$ might become shorter and charged at high dielectric constant environments. The D33 experiments continued this work to paint a more complete picture. Additionally the efforts were focused towards studying the system under catalytic conditions. The aim of the experiment was to determine whether there is any change in the catalyst $\mathbf{((1)_4)_n}$ structure during a 'live' catalytic reaction or once the substrate is exhausted.

Results and Discussion

Structure vs solvents

^{31}P NMR data analysis suggested that the oligomeric structure of palladium(II) Trost complex, **((1)$_4$)$_n$** in various solvents may differ significantly. Dielectric constant, ε_r was identified as a key solvent parameter.

The importance of the dielectric constant, ε_r for charged particle separation is demonstrated by *Bjerrum length* equation:

$$\lambda_B = \frac{e^2}{4\pi\varepsilon_0\varepsilon_r k_B T}$$

The separation distance, λ_B is inversely proportional to the dielectric constant of the media in which the solute is dissolved. The equation presumes point charges, however the general principles may still apply to more complex systems such as **1**. For example, ion-ion separation is favoured in polar solvents such as water or DMSO, but becomes increasingly difficult in less polar aprotic organic solvents. Aggregation phenomenon may be closely related extension to this simple model, where multiple close range electrostatic interactions can minimise the overall system energy. Precipitation out of solution could be considered the most extreme case of aggregation.

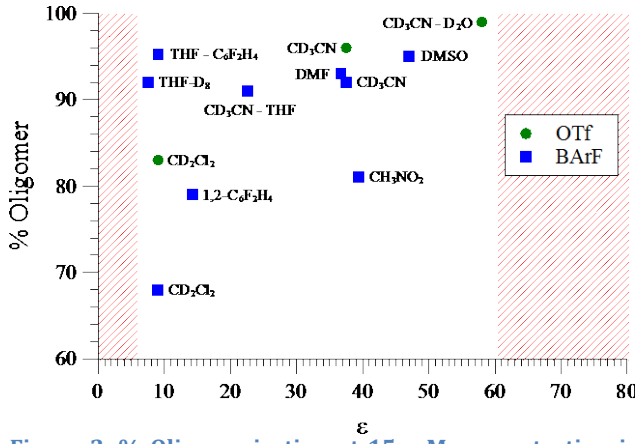


Figure 2. % Oligomerisation at 15 mM concentration in various solvent mixtures as determined by ^{31}P NMR; red areas indicate insoluble mixtures.

The complex **1-BArF** is highly soluble in solvents such as THF (ε_r = 7.6) or dichloromethane (ε_r = 9.1) where the oligomers are the dominating species, ***Figure 2***. Less polar solvents, including hexane, benzene, hexafluorobenzene or diethyl ether are known to cause oiling out, or precipitation of the catalyst **1** as amorphous solid. On the other end of the polarity scale, the levels of aggregation in both acetonitrile (ε_r = 37.5) and DMSO (ε_r = 47) are significantly reduced, ***Figure 3a***. Very short flexible cylinders (r ≈ 7 Å; L ≈ 30 Å) were detected by SANS in dilute solutions. The material is not soluble in water or any aqueous mixtures, while in a mixture of THF and acetonitrile (ε_r ≈ 23) as expected the compound forms medium length cylinders.

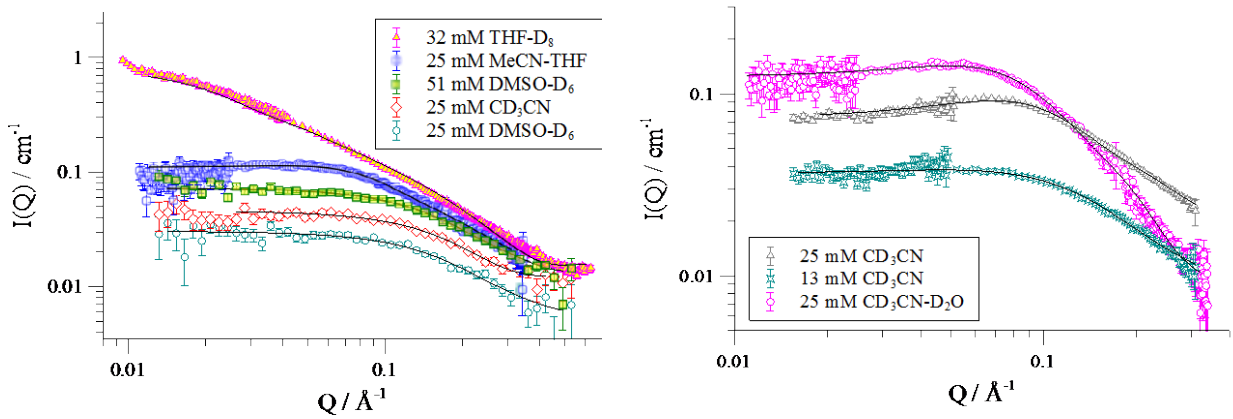


Figure 3. a) left: 1-BArF oligomers in selected solvent mixtures; b) right: 1-OTf oligomers in MeCN-D_3 and MeCN-D_3/D_2O mixtures, 25 ^{0}C, ILL-D33

The triflate complex **1-OTf** behaves slightly differently. It is insoluble in THF, and instead forms up to 330 Å long semi-flexible cylinders in CH_2Cl_2. The anion effect becomes even more pronounced in higher dielectric constant solutions. The SANS data indicates the presence of charged particles in acetonitrile based mixtures (ε_r = 47-58), ***Figure 3b***. The polar solvent is capable of stabilising triflate anion in the presence of positively charged palladium(II) rich oligomer cores. The ion-ion separation and charge repulsion interactions lead to the formation of much shorter aggregates of around 30 Å length. However, it is still clear that the solutions remain dominated by oligomers regardless of their underlying architecture.

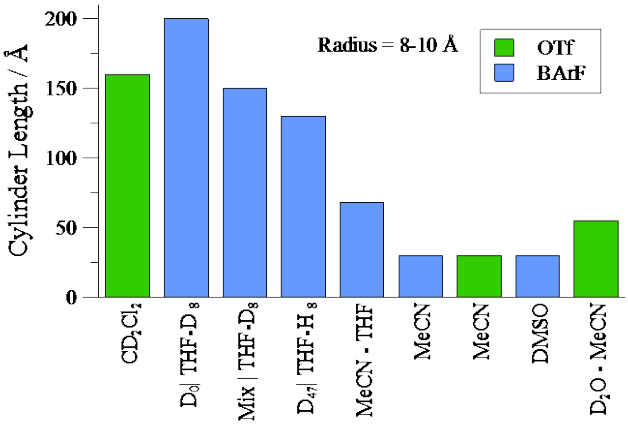


Figure 4. SANS Cylinder length of selected 1-BArF and 1-OTf samples